Final Draft

of the original manuscript:

Lozano, G.A.; Na Ranong, C.; Bellosta von Colbe, J.M.; Bormann, R.;
Hapke, J.; Fieg, G.; Klassen, T.; Dornheim, M.:

Optimization of hydrogen storage tubular tanks based on light weight hydrides

In: International Journal of Hydrogen Energy (2011) Elsevier

DOI: 10.1016/j.ijhydene.2011.03.043

Optimization of hydrogen storage tubular tanks based on light weight hydrides

Gustavo A. Lozano[a,*], Chakkrit Na Ranong[b], Jose M. Bellosta von Colbe[a], Rüdiger Bormann[a], Jobst Hapke[b], Georg Fieg[b], Thomas Klassen[a], Martin Dornheim[a]

[a] Institute of Materials Research, Materials Technology, Helmholtz-Zentrum Geesthacht, D-21502 Geesthacht, Germany

[b] Institute of Process and Plant Engineering, Hamburg University of Technology, D-21073 Hamburg, Germany

Abstract

Design of hydrogen storage systems aims at minimal weight and volume while fulfilling performance criteria. In this paper, the tubular tank configuration for hydrogen storage based on light weight hydrides is optimized towards its total weight using the predictions of a newly developed simulation model. Sodium alanate is taken as model material. A clear definition of the optimization is presented, stating a new optimization criterion: a defined total mass of hydrogen has to be charged in a given time, instead of prescribing percentages of the total hydrogen storage capacity. This yields a wider space of possible solutions. The effects of material compaction, addition of expanded graphite and different tubular tank diameters were evaluated. It was found that compaction of the material is the most influential factor to optimize the storage system. In order to obtain lighter storage systems one should concentrate on improving the ratio mass of hydride bed to mass of tank wall by screening lighter materials for the tank wall and developing hydrogen storage materials exhibiting both higher gravimetric and volumetric storage capacities.

[*] Corresponding author Tel.: +49 41 5287 2643; fax: +49 41 5287 2625. Email address: gustavo.lozano@hzg.de (Gustavo A. Lozano)

1 Introduction

Design of hydrogen storage systems aims at minimizing the total required volume and weight while fulfilling performance criteria such as total storage capacities, charging times, delivery rates, driving ranges in automobile applications [1, 2]. With higher volumetric storage capacity, hydrogen storage in metal hydrides offers an alternative to compressed hydrogen storage (pressure up to 700 bar) or liquid hydrogen storage (temperature down to 20 K). For instance, the complex ternary hydride Mg_2FeH_6 has the highest known hydrogen volumetric density, 150 kg H_2 m^{-3} [3], which is more than twice the density of liquid hydrogen and three times that of hydrogen gas under 1000 bar. Bringing metal hydrides from milligram-scale investigations into kilogram-scale applications involves challenges in the material production [4, 5] and in the realization of the sorption process. Concerning the sorption process, in every hydrogen storage system based on metal hydrides, no matter the size or scale, three sub-processes occur inside the hydride bed during hydrogen sorption: hydrogen transport, chemical reaction and heat transfer. Hydrogen transport and heat transfer do not usually restrict the sorption process in small scale systems, and this should be guaranteed if it is desired that the only sub-process to be evaluated is intrinsic kinetics (chemical reaction). On the other hand, in large scale geometries heat transfer is usually the rate limiting sub-process and thus engineering design of the storage system is mainly oriented towards heat transfer requirements.

The final targets of research and development of metal hydride scale-up are focused on automobile applications. The first car reported using metal hydrides as storage media was built by Billings Energy Research Corporation in 1976 using a TiFe alloy [6, 7]. In the late 70's and in the 80's Daimler extensively developed and constructed metal hydride storage systems based on the intermetallic alloy $Ti_{0.98}Zr_{0.02}V_{0.45}Fe_{0.1}Cr_{0.05}Mn_{1.5}$ and TiFe alloy for a fleet of vans with demonstration purposes [8-10]. Central considerations were given to the heat transfer, in which a tubular tank configuration was implemented. For comparison purposes, this system could be considered as the standard metal hydride-based storage system for automobile applications, having a reported hydrogen capacity of around 1 wt% and 29 kg H_2 m^{-3} [8, 11]. In order to achieve lower system weights other hydrogen storage materials with higher gravimetric capacities are being investigated.

In complex hydride development, Bogdanovic and Schwickardi showed that hydrogen can be reversibly stored in and released from sodium alanate if doped with titanium compounds [12]. Sodium alanate, $NaAlH_4$, is reversibly formed in a two-step reaction from NaH and Al within the technically favorable conditions of up to 100 bar and 125 °C (see Eq. 4 and 5). It has a theoretical gravimetric hydrogen storage capacity of 5.6 wt%, enabling possible higher gravimetric capacities in comparison to conventional metal hydrides. The group of compounds taking part in these equations, which is sometimes also called Na-Al-H system, will be referred in this investigation as sodium alanate material. Sodium alanate has been selected as scale-up model material to understand and manage

possible hurdles in the development of storage systems based on light weight metal hydrides. An 8 kg sodium alanate storage tank was designed and constructed in a close collaboration of the Helmholtz-Zentrum Geesthacht and the Hamburg University of Technology by Na Ranong et al in the frame of the STORHY project [1, 13] and is currently under evaluation by Bellosta von Colbe et al [14]. It is based on loose powder and optimized toward the charging time of the system. In a different approach, Mosher et al designed and constructed a sodium alanate based hydrogen storage system, evaluating safety and component optimization. Two different configurations, also loose powder based, were considered, the first one equipped with an open celled aluminum foam for heat transfer enhancement and a second one with finned tube design and using a special developed filling procedure applying biaxial vibration to enhance powder densification and loading of the system [15]. .In a joint project, Sandia and GM Corporation developed, constructed and evaluated a sodium alanate tank based on the shell and tube configuration, implementing a cost-efficient design with automated operation [16, 17]. In addition, the feasibility of an on-board hydrogen storage system for automotive applications using sodium alanate and $Ti_{1.1}CrMn$ alloy was examined using numerical simulations [18, 19].

The present investigation proposes and discusses an optimization procedure to determine metal hydride storage systems with minimal weight, the case study selected is sodium alanate material and the tubular tank configuration, as presented in Fig. 1. This configuration can correspond to a double pipe design or to a shell and tube design, in which heat transfer fluid is flowing around the tubular tank for cooling/heating purposes. The optimization process is based on predictions of a simulation tool developed and validated for the hydrogen sorption of sodium alanate material (see appendix). The experimental work on which the analysis of this present work is based (material preparation, kinetics modeling, compaction effects, tank sorption measurements) is presented elsewhere [20]. Two material modifications that have the potential to improve the performance of the system are taken in consideration in this analysis: compaction of the active material and addition of expanded graphite (EG) to the active material for thermal conduction enhancement. Optimizations of tubular tanks filled with loose powder and with compacted material are compared. Compacted material has the advantage of higher volumetric hydrogen density and higher thermal conductivity if compared to loose powder. Nevertheless, the permeability to flow decreases and the volumetric heat release from the hydrogenation is higher. Beyond the possible improvement by compaction, the addition of EG is also evaluated in the optimizations. This addition enhances the effective thermal conductivity of the hydride bed, although increasing the amount of inert mass in the system and thus diminishing the total hydrogen storage capacity.

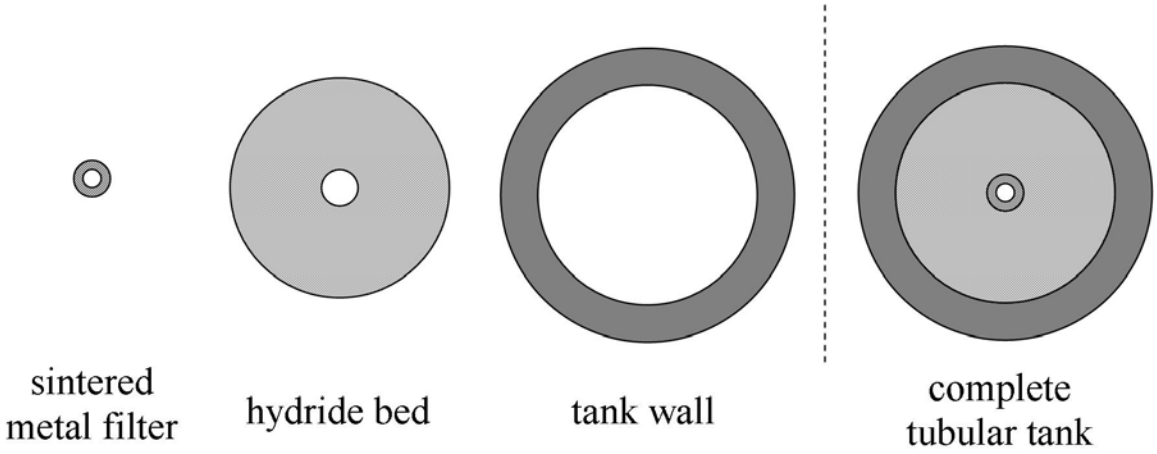

Fig. 1: Cross-section of a tubular tank filled with sodium alanate material.

2 Definition of the tank optimization task

The design of a storage system depends strongly on its defined goal function and constraints. Therefore it is essential that the definition of any design is clearly stated for development, comparison, and improvement purposes. In this investigation the system is optimized towards its weight. Optimization is the process of finding the maximum (or minimum) value of a function, by changing the values of a set of variables. Simultaneously, predefined criteria (constraints and conditions) must be fulfilled. Table 1 summarizes how the optimization of a tubular storage tank based on sodium alanate is defined in the present work: function to be optimized, variables, and constraints and conditions. A new optimization criterion is proposed: a defined total mass of hydrogen (for this work 4.5 kg) has to be charged in a given time, instead of prescribing percentages of the total hydrogen storage capacity, as it is done in other investigations [8, 13]. This new definition does not restrict the total mass of the absorbing material and offers a wider solution space for the optimization, even ensuring at least the optimum that is found when the percentage of the total capacity is fixed as condition.

Within the scope of the optimization the total weight of the hydrogen storage system is composed of the weights of the tank wall, the hydride bed and the sintered metal filter (Fig. 1). End caps are not considered. For different internal diameters of the tank, D_i, the total length of the tubular tank is calculated, in order to satisfy both the time charging condition and the total capacity of the tubular tank (conditions 3 and 4 of Table 1): Eq. 1 ensures that at least the mass $m_{\mathrm{H_2},10\mathrm{min}}$ is filled within 10 min (left argument of the maximum function) and simultaneously the minimal capacity of the storage system $m_{\mathrm{H_2},tot}$ is fulfilled (right argument of the maximum function). Only the hydrogen absorbed in the material is considered. In the case of the present optimization $m_{\mathrm{H_2},10\mathrm{min}}$ is defined to

4.5 kg and $m_{\mathrm{H}_2,tot}$ to 5 kg. The diameter of the sintered metal filter D_{sf} is fixed to 6 mm. The main role of the predictions from the simulation tool is the determination of $w_{10\,\mathrm{min}}$, the mass of hydrogen absorbed after 10 min per mass of material. The values of bulk density, ρ_b, and total capacity of the material, w_{tot}, are conditioned to the physical state of the sodium alanate material used and are discussed in subsection 2.2. The total length of the tubular tank is the given as L by Eq. 1.

$$L = \max\left(\frac{10^6 m_{\mathrm{H}_2,10\,\mathrm{min}}}{\rho_b w_{10\,\mathrm{min}} \frac{\pi}{4}\left(D_i^{\,2} - D_{sf}^{\,2}\right)}, \frac{10^6 m_{\mathrm{H}_2,tot}}{\rho_b w_{tot} \frac{\pi}{4}\left(D_i^{\,2} - D_{sf}^{\,2}\right)} \right) \tag{1}$$

It is important to stress, that the calculated total length of the tank corresponds to the sum of the length of possible individual tubular tanks (e.g. in a bundle shell and tube design). The number of individual tanks would be defined by the total required length and the limit on how long each individual tank could be. The definition of number of tanks and the length of each individual tank is not within the scope of this investigation.

Both selected design temperature and design pressure condition the required thickness of the tubular tank wall, see subsection 2.1. The total weight of the tubular tank is then calculated from the diameters of the sintered metal filter, internal and external diameter of the tubular tank, densities of the materials and the required length determined by Eq. 1. The physical and transport properties of sodium alanate material (as loose powder, as compacted material and as compacted material with the addition of EG), which are required in the simulation predictions, are discussed in subsection 2.2.

Table 1: Optimization definition for a tubular tank based on sodium alanate material

Issue	Definition
Function to be minimized	Weight of the hydrogen storage system
Variables	1. Internal diameter of the tubular tank 2. Compaction level 3. Addition of EG
Conditions and constraints	1. The basic configuration of the tubular tank is as presented in Fig. 1 2. Hydrogen storage based on sodium alanate material, prepared as presented in [20] 3. Time to charge 4.5 kg H_2: 10 min 4. Total hydrogen capacity of the storage system ≥ 5 kg H_2 5. Tank wall material is standard stainless-steel 1.4571 for hydrogen applications. 6. Absorption pressure: 100 bar 7. Calculation pressure for tank wall thickness is 100 bar 8. Calculation temperature for tank wall thickness is 250 °C

2.1 Calculation of the tank wall thickness

The thickness of the tubular tank must hold the stresses due to the hydrogen pressure, which are highest during hydrogenation. The tank wall thickness is calculated according to the technical specifications of the codes of practice on pressure vessels AD 2000 [21]. The material of the wall is the standard stainless-steel 1.4571, suitable for hydrogen applications. Eq. 2 is the basis of the wall thickness calculation for cylinders [21]. By using this expression, the tank wall thickness and the external diameter of the tubular tank are determined for a specific internal diameter.

$$s = \frac{D_a p}{20\frac{K}{S} + p} \tag{2}$$

In Eq. 2, s is the required wall thickness [mm], D_a the external diameter of the tubular tank [mm], p the design pressure [bar], K the design strength value of the wall material [N mm^{-2}], S the design

safety factor [-]. The design strength value of standard stainless-steel 1.4571 is taken as 186 N mm^{-2} at 250 °C. Further details of the calculation procedure and the values of the parameters can be found in the cited reference [21]. Table 2 presents the values of wall thickness for different tank diameters.

2.2 Physical and transport properties of the hydride bed

Both physical and transport properties of the hydride bed, such as bulk density, thermal conductivity and permeability, are parameters of the system which have a central role in the modeling and optimization of the storage system. This subsection summarizes the values assumed for these properties in the simulations and how they are affected by the compaction process and the addition of EG.

The loose sodium alanate material used in this investigation has a bulk density of 600 kg m^{-3} and a thermal conductivity of 0.8 W m^{-1} K^{-1} [22]. According to the experimental results on the kinetics of the loose sodium alanate material its total hydrogen storage capacity is 3.9 wt% [23, 24]. The permeability of the loose powder is 3.17×10^{-13} m^2 [11].

Table 2: Calculated wall thickness for different tubular tank diameters. The design pressure and temperature are 100 bar and 250 °C, respectively. The material is the austenitic stainless-steel 1.4571. Design safety factor S = 1.5.

Internal diameter [mm]	**Calculated wall thickness [mm]**	**External diameter [mm]**
20	1.3	22.6
40	2.6	45.2
60	3.9	67.7
80	5.2	90.3
100	6.4	112.9

Compaction of loose powder beds leads to a significant improvement of the effective thermal conductivity [25, 26]. From the results of compaction of magnesium hydride [26], in which the thermal conductivity is increased by a factor of 3 when compared to loose material, a thermal conductivity of 2 W m^{-1} K^{-1} is expected for the compacts of sodium alanate material. Even higher

enhancement is reported for conventional metal hydrides [27]. According to our experimental results, the bulk density of the compacts after cycling is 1100 kg m^{-3} and its total hydrogen storage capacity 4.5 wt% [20]. In order to estimate the change of the permeability by compaction and reduction of the porosity (from a compacted state 1 to a compacted state 2), the Blake-Kozeny equation is implemented:

$$\kappa_2 = \kappa_1 \left(\frac{\varepsilon_2}{\varepsilon_1} \right)^3 \left(\frac{1-\varepsilon_1}{1-\varepsilon_2} \right)^2 \tag{3}$$

Addition of EG to metal hydride material leads to a significantly improved thermal conductivity for loose sodium alanate powder. This is reported for metal hydrides compacts [25-28]. Compacts of magnesium hydride with of 5 wt% EG have a thermal conductivity of 4 W m^{-1} K^{-1} and with 10 wt% the thermal conductivity goes up to a value of 7 W m^{-1} K^{-1} [26]. These effective thermal conductivities are taken for the simulation predictions of sodium alanate compacts with EG. The additional inert EG in the compacts reduces the total hydrogen storage capacity of the material: from 4.5 wt% to 4.3 wt% if 5 wt% EG is added, and to 4.05 wt% with an addition of 10 wt% of EG. Changes of the bulk density and permeability by the addition of EG are neglected.

2.3 Simulation model

Since pressure, temperature and composition may depend upon the spatial location in a hydride bed during a hydrogen sorption process as a consequence of the coupled transport phenomena (heat transfer and hydrogen transport) with chemical reaction, numerical simulations are required to solve the model equations that describe the coupled sub-processes of hydrogen transport, intrinsic kinetics and heat transfer in physical geometries. The role of the simulation in the frame of the present optimization is the prediction of the total hydrogen mass absorbed after 10 min, $w_{10\,\mathrm{min}}$ (Eq. 1). The implemented governing equations to describe the absorption process of sodium alanate and further details of the simulation are presented in the appendix. A new approach to follow the reaction kinetics of sodium alanate and thus the mass concentration of the reacting species is proposed, implementing an empirical kinetic model developed for the sodium alanate material on which this investigation is based [23]. The proposed modeling approach is not restricted to sodium alanate material and is also suitable for simulation of other metal hydride systems.

3 Results

The absorption behavior of tubular tanks of different internal diameters was simulated for loose powder, compacts and compacts with addition of EG. The results are summarized in Fig. 2. In the

simulations both heat transfer fluid temperature and initial system temperature were 110 °C. An important parameter in the simulations is the value of the heat transfer coefficient at the tubular tank external surface, which depends on the tubular diameter, geometric arrangement, flow conditions, and the properties of the heat transfer fluid. For the evaluations, a constant heat transfer coefficient of 500 W m^{-2} K^{-1} is assumed at the tubular tank external surface. The total system weight according to the conditions of the optimization is calculated and plotted as a function of the tank internal diameter, Fig. 3. There is a diameter which has a minimum weight of system for each type of material. For loose powder, the minimum total system weight is 640 kg for a tubular tank with an internal diameter of 35 mm. In the case of compacts, with and without EG addition, the minimum system weight is between 350 and 400 kg.

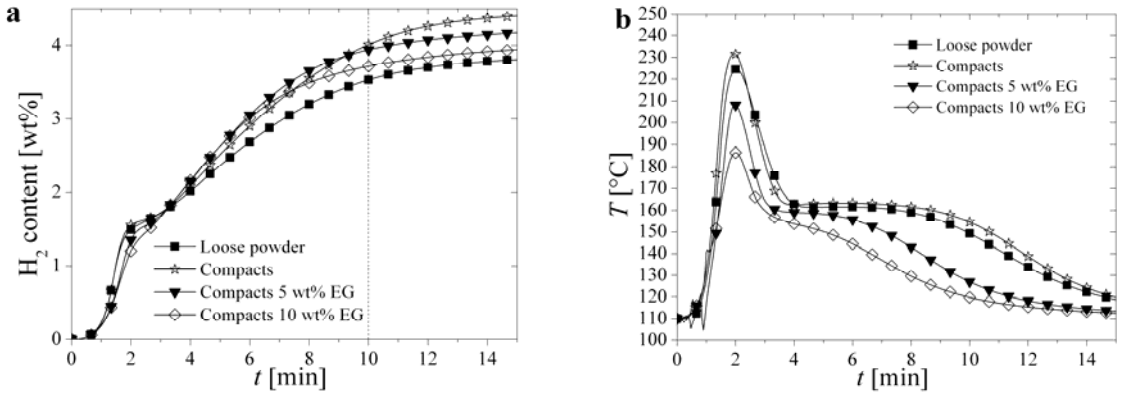

Fig. 2: Predicted profiles of hydrogen content (a) and temperature close to the sintered filter (b) of a tubular storage tank with D_i = 35 mm filled with sodium alanate material. The conditions and constraints are presented in Table 1. The temperature of the heat transfer fluid and the initial temperature of the system is 110 °C. The heat transfer coefficient of the heat transfer fluid side is 500 W m^{-2} K^{-1}

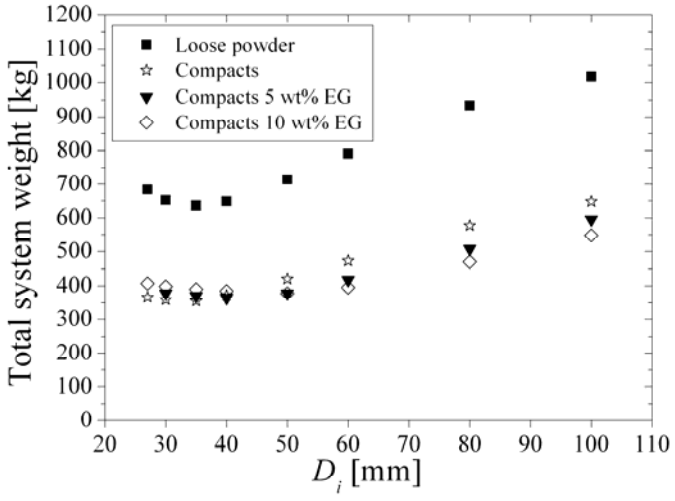

Fig. 3: Calculated system weight of a tubular storage tank filled with sodium alanate material as a function of the internal diameter. The conditions and constraints are presented in Table 1. The temperature of the heat transfer fluid and the initial temperature of the system is 110 °C. The heat transfer coefficient of the heat transfer fluid side is 500 W m^{-2} K^{-1}

4 Discussion

There are two contrary effects that explain that optimal diameters with minimum total system weight occur for each material in Fig. 3. First, as the internal tank diameter is increased, the ratio of mass of hydride bed to mass of tank wall, $m_{\text{Hydride Bed}}/m_{\text{Tank Wall}}$, also increases. Consequently, less inert material (tank wall) per mass of active material is added to the system. The ratio $m_{\text{Hydride Bed}}/m_{\text{Tank Wall}}$ is calculated from the internal and external diameters of the tubular tank, the cross sectional area of the tank, and the densities of the wall and the material. Fig. 4 shows the calculated ratio $m_{\text{Hydride Bed}}/m_{\text{Tank Wall}}$ for loose material and compacted material as a function of the internal tank diameter. The ratio is 0 when there is no space for the hydride material, i.e. when the internal tank diameter is equal to the diameter of the sintered filter, 6 mm. The ratio increases quite fast for internal diameters from 10 mm to 40 mm. For larger diameters the ratio tends asymptotically to a constant value. No noticeable enhancement is observed for internal diameters larger than 70 mm, e.g. less than 1 % enhancement in the ratio $m_{\text{Hydride Bed}}/m_{\text{Tank Wall}}$ is obtained if the diameter goes up to 500 mm. There is an opposed effect when the internal diameter is increased: the resistance to heat transfer and hydrogen transport becomes larger. As a result, the hydrogen content in the hydride bed after 10 min

may be diminished at larger diameters. These two contrary effects lead to an optimal tank diameter, which for the present analysis is around 40 mm according to Fig. 3.

Fig. 4 clarifies why the total weight of system for compacted material is much lower than for loose material in Fig 3. The lower weight of the storage system filled with compacts is explained by the larger bulk density of the compacted material, which causes a larger ratio mass of hydride bed to mass of tank wall in comparison to the loose powder. In addition, as experimentally shown for the material on which this investigation is based [20], the hydrogen content of loose powder (3.9 wt%) is lower than the one of compacted material (4.5 wt%). Compaction of sodium alanate material causes a total reduction of almost 45 % of the weight of a tubular storage tank, when compared to loose powder. The low permeability of the compacted material did not cause any detrimental effect in the absorption behaviour. The predicted pressure gradients that were developed in the hydride bed were quite low for all types of material.

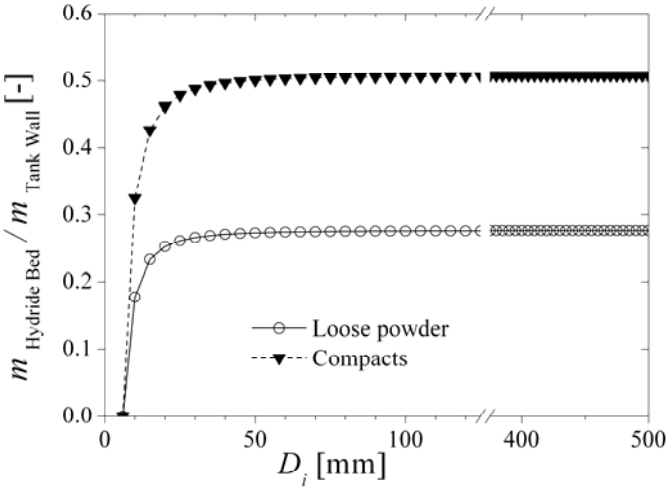

Fig. 4: Ratio of mass of hydride bed to mass of tank wall as a function of the internal diameter of the tubular tank. The ratio for compacts refers to material with and without addition of EG.

The additional EG in the compacted material did not achieve lower optimal system weights (Fig. 3). It was expected that the enhanced thermal conductivity through the additional EG would lead to optimal diameters with less total system weight, since the heat transfer resistance is diminished. The enhancement of the thermal conduction throughout the hydride bed is reflected in the temperature profiles, Fig. 2b. The temperature in Fig. 2b corresponds to a position close to the sintered filter and where the hottest spots of temperature were detected in the hydride bed. The lowest and shortest temperature peaks are found for the material with the addition of EG. Although not considered in the present optimization, lower levels and peaks of temperature could bring some advantages for the tank

design. First, it would be possible to have tank designs with thinner walls and options to selection of other lighter wall materials with higher strength (which have a better performance and are more suitable at lower temperatures). Another advantage of operating the system at lower temperature levels is that it reduces the risk of possible methane formation by the interaction of the carbon with hydrogen in the presence of transition metal catalysts [29, 30]. In addition, the risk of the melting of $NaAlH_4$ (melting point 183 °C [31]) is also reduced. However, it must be pointed out that at the operating pressure of 100 bar the equilibrium temperature for the second step of hydrogenation (Eq. 5) is around 170 °C [32]. If the hydride bed reaches a temperature higher than 170 °C after the first step of reaction, the formation of $NaAlH_4$ should not proceed until the temperature of the material has decreased significantly below that temperature. This should cause a delay between the two absorption steps [22] and conditions for melting of $NaAlH_4$ should not be present.

Only at diameters > 40 mm it is observed that the weight of the system is the lowest for compacted material with 5 or 10 wt% EG. Nevertheless, the overall minimal total system weight is obtained with the compacted material without any addition of EG in a tubular tank of D_i =35 mm. The additional EG reduces the active material in the tank and therefore more weight is added to the system (see the final hydrogen contents achieved in Fig. 2a). Moreover, larger diameters do not enhance the ratio mass of hydride to wall mass enough to compensate the additional inert EG (Fig. 4).

Further optimizations were performed by changing the operating conditions, Figs. 5 and 6. The initial temperature and the thermal oil temperature are set to 130 °C. In addition, the heat transfer coefficient is changed to 5000 W m^{-2} K^{-1}. No significant change is obtained in the minimum total system weights: minimum total system weight is still around 640 kg for loose powder and around 350 and 400 kg for compacted material with and without EG. Further enhancement of the heat transfer coefficient does not diminish the total weight of the system. Evaluations of hydrogen pressures during absorption other than 100 bar were not in the scope of the present optimization.

The corresponding gravimetric and volumetric capacities of the calculated optimal alanate hydrogen storage system are 0.014 kg_{H_2} kg_{System}^{-1} and 0.038 kg_{H_2} l_{System}^{-1}, respectively. This optimal system has still a higher energy density (2 MJ kg^{-1}, 6 MJ l^{-1}) when compared to lead-acid batteries (0.1 MJ kg^{-1}, 0.4 MJ l^{-1}), nickel-metal hydride batteries (0.4 MJ kg^{-1}, 1.6 MJ l^{-1}) and Lithium-ion batteries (0.6 MJ kg^{-1}, 1 MJ l^{-1}) [33]. Nevertheless, it must be pointed out that the reported energy density of the alanate hydrogen storage system does not include the additional weight and volume of the fuel cell system. Achieving lighter storage systems should concentrate on improving the ratio $m_{\text{Hydride Bed}}/m_{\text{Tank Wall}}$ and the hydrogen storage capacity of the hydride bed. For instance, the hydrogen capacity of the sodium alanate material of this work could be enhanced and optimized by eliminating the carbon addition during milling [20], which may be not crucial for kinetics but is

adding inert material to the system. The excess aluminum in the material, which is adding inert mass to the reacting system as well, can be also optimized: using the exact stoichiometric amount or different excess aluminum amounts (e.g. considering the possible consumption of aluminum by reacting with titanium), which should bring benefits for hydrogenation kinetics and hydrogen capacity of the material [34]. Another feasible option for lighter storage systems is the evaluation of lighter and hydrogen resistant materials for the tank wall other than the heavy stainless steel (e.g. aluminum alloys, titanium alloys). Materials compatibility studies of sodium alanate with aluminum pressure tanks [35] showed that the integrity of the tank is compromised by the interaction of the tank material with the alanate during cycling (aluminum is consumed in the reverse hydride-formation reactions). Potential materials for the pressure tank are light titanium alloys, e.g. $Ti_5Al_{2.5}Sn$, which have been employed as hydrogen tanks and pressure vessels [36]. Since there are not known results with alanate, material compatibility analysis should be done in order to prove that there is no interaction between the material and the alanate. In addition, the effect of hydrogen pressure other than 100 bar on the sorption could also lead to lower system weights.

Furthermore, hydrogen storage materials exhibiting both higher gravimetric and volumetric storage capacity are required in order to achieve lighter storage systems.

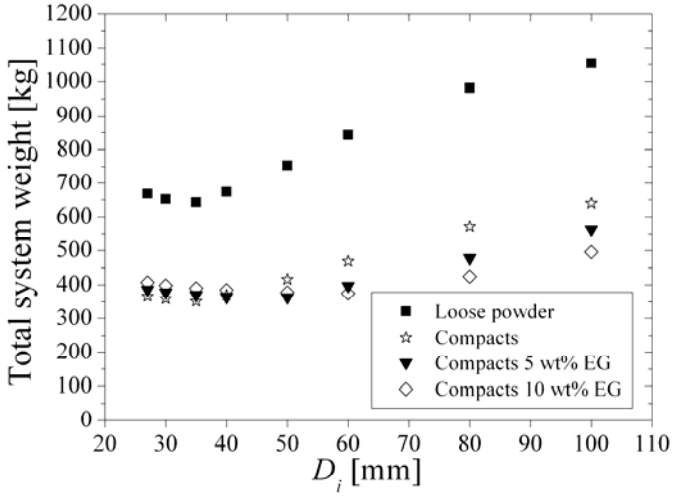

Fig. 5: Calculated system weight of a tubular storage tank filled with sodium alanate material as a function of the internal diameter. The conditions and constraints are presented in Table 1. The initial and oil temperature is 130 °C. The heat transfer coefficient at the oil side of the tubular tank is set to 5000 W m^{-2} K^{-1}

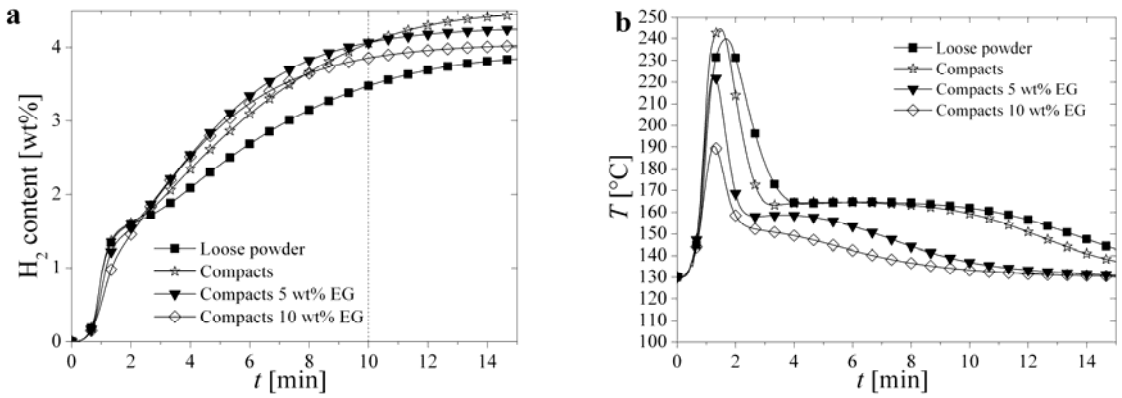

Fig. 6: Predicted profiles of hydrogen content (a) and temperature close to the sintered filter (b) of a tubular storage tank with D_i = 35 mm filled with sodium alanate material. The conditions and constraints are presented in Table 1. The initial and oil temperature is 130 °C. The heat transfer coefficient at the oil side of the tubular tank is set to 5000 W m^{-2} K^{-1}

5 Conclusions

The tubular tank configuration for hydrogen storage based on light weight hydrides, taking sodium alanate as model material, was theoretically optimized towards its total weight. Essential for the applied procedure was to state a clear definition of the optimization: function to be optimized, variables to be evaluated, as well as conditions and constraints. A new concept in the charging condition was proposed: a defined total mass of hydrogen has to be charged in a given time, instead of prescribing percentages of the total hydrogen storage capacity. This new definition does not restrict the total mass of the absorbing material and offers a wider space of solutions for the optimization, even ensuring at least the optimum found when a percentage of the total capacity is fixed as time-charging condition. The optimization process included the evaluation of material compaction, the addition of EG and different tank diameters. It was found that compaction of the material is the most influential factor to optimize the hydrogen capacity of the storage system. Achieving lighter systems should concentrate on improving the ratio $m_{\text{Hydride Bed}} / m_{\text{Tank Wall}}$ and the hydrogen storage capacity of the hydride bed. For instance, the hydrogen capacity of the sodium alanate material of this work could be enhanced by eliminating the carbon addition during milling and the excess aluminium in the material. Another feasible option is to evaluate lighter and hydrogen resistant materials for the tank wall other than the standard heavy stainless steel for hydrogen applications. Furthermore, hydrogen storage materials exhibiting both higher gravimetric and volumetric storage capacity are required in order to achieve lighter storage systems.

Acknowledgments

The authors appreciate the financial support of the European Community in the frame of the Integrated Project "NESSHY—Novel Efficient Solid Storage for Hydrogen" (contract SES6-CT-2005-518271) and of the Helmholtz Initiative "FuncHy—Functional Materials for Mobile Hydrogen Storage".

References

[1] StorHy. StorHy Final Publishable Activity Report. 2008. http://www.storhy.net/pdf/StorHy_FinalPublActivityReport_FV.pdf; [viewed 02.10.2009]

[2] US Department of Energy. Targets of onboard hydrogen storage systems. http://www1.eere.energy.gov/ohydrogenandfuelcells/storage/pdfs/targets_onboard_hydro_storage.pdf; [viewed 12.02.2010]

[3] Schlapbach L, Züttel A. Hydrogen-storage materials for mobile applications. Nature 2001;414:353-358.

[4] Eigen N, Keller C, Dornheim M, Klassen T, Bormann R. Industrial production of light metal hydrides for hydrogen storage. Scripta Mater. 2007;56:847-851.
[5] Dornheim M, Eigen N, Barkhordarian G, Klassen T, Bormann R. Tailoring Hydrogen Storage Materials Towards Application. Advanced Engineering Materials 2006;8:377-385.
[6] Ludwig Bölkow Systemtechnik. Hydrogen and Fuel Cell Vehicles Worldwide. 2010. http://www.netinform.net/H2/H2Mobility/Default.aspx; [viewed 18.11.2010]
[7] Roger E. Billings. Milestones Roger E. Billings. 2010. http://www.rogerebillings.com/Timeline/Timeline.html; [viewed 18.11.2010]
[8] Alternative Energien für den Straßenverkehr - Wasserstoffantrieb in der Erprobung / Hrsg.: Projektbegleitung Kraftfahrzeuge u. Strassenverkehr, TÜV Rheinland e.V. Im Auftrag d. Bundesministeriums für Forschung u. Technologie Köln: Verlag TÜV Rheinland, 1989.
[9] Buchner H, Povel R. The daimler-benz hydride vehicle project. Int. J. Hydrogen Energy 1982;7:259-266.
[10] Buchner H. The hydrogen/hydride energy concept. Int. J. Hydrogen Energy 1978;3:385-406.
[11] Franzen J. Modellierung und Simulation eines Wasserstoffspeichers auf der Basis von Natriumalanat. VDI-Fortschrittsberichte, 6 (583), VDI-Verlag, Düsseldorf 2009.
[12] Bogdanovic B, Schwickardi M. Ti-doped alkali metal aluminium hydrides as potential novel reversible hydrogen storage materials. J. Alloys Compd. 1997;253-254:1-9.
[13] Na Ranong C, Höhne M, Franzen J, Hapke J, Fieg G, Dornheim M, Eigen N, Bellosta von Colbe JM, Metz O. Concept, Design and Manufacture of a Prototype Hydrogen Storage Tank Based on Sodium Alanate. Chemical Engineering & Technology 2009;32:1154-1163.
[14] Bellosta von Colbe JM, Metz O, Lozano GA, Pranzas PK, Schmitz HW, Beckmann F, Schreyer A, Klassen T, Dornheim M. Behaviour of scaled-up sodium alanate hydrogen storage tanks during sorption. To be published 2010.
[15] Mosher DA, Arsenault S, Tang X, Anton DL. Design, fabrication and testing of NaAlH4 based hydrogen storage systems. J. Alloys Compd. 2007;446-447:707-712.
[16] Johnson TA, Jorgensen S, Dedrick DE. Performance of a Full-Scale Hydrogen-Storage Tank Based on Complex Hydrides. Faraday Discussions 2011;151:in review.
[17] Johnson TA, Kanouff MP, Dedrick DE, Evans G, Jorgensen S. Model-based Design of an Automotive-scale Metal Hydride Hydrogen Storage System. IJHE Special Issue: AIChE 2010, June, 2011: in review.
[18] Raju M, Kumar S. System simulation modeling and heat transfer in sodium alanate based hydrogen storage systems. Int. J. Hydrogen Energy 2011;36:1578-1591.
[19] Raju M, Ortmann JP, Kumar S. System simulation model for high-pressure metal hydride hydrogen storage systems. Int. J. Hydrogen Energy 2010;35:8742-8754.
[20] Lozano GA. Development of Hydrogen Storage Systems using Sodium Alanate. Dissertation. Technische Universität Hamburg-Harburg, Hamburg 2010.
[21] AD 2000 Regelwerk. Berlin: Verband der TÜV e.V., 2008.
[22] Lozano GA, Eigen N, Keller C, Dornheim M, Bormann R. Effects of heat transfer on the sorption kinetics of complex hydride reacting systems. Int. J. Hydrogen Energy 2009;34:1896-1903.
[23] Lozano GA, Na Ranong C, Bellosta von Colbe JM, Bormann R, Fieg G, Hapke J, Dornheim M. Empirical kinetic model of sodium alanate reacting system (I). Hydrogen absorption. Int. J. Hydrogen Energy 2010;35:6763-6772.
[24] Lozano GA, Na Ranong C, Bellosta von Colbe JM, Bormann R, Fieg G, Hapke J, Dornheim M. Empirical kinetic model of sodium alanate reacting system (II). Hydrogen desorption. Int. J. Hydrogen Energy 2010;35:7539-7546.

[25] Rodríguez Sánchez A, Klein H-P, Groll M. Expanded graphite as heat transfer matrix in metal hydride beds. Int. J. Hydrogen Energy 2003;28:515-527.
[26] Chaise A, de Rango P, Marty P, Fruchart D, Miraglia S, Olivès R, Garrier S. Enhancement of hydrogen sorption in magnesium hydride using expanded natural graphite. Int. J. Hydrogen Energy 2009;34:8589-8596.
[27] Klein H-P, Groll M. Heat transfer characteristics of expanded graphite matrices in metal hydride beds. Int. J. Hydrogen Energy 2004;29:1503-1511.
[28] Kim KJ, Montoya B, Razani A, Lee KH. Metal hydride compacts of improved thermal conductivity. Int. J. Hydrogen Energy 2001;26:609-613.
[29] Espinal JF, Mondragón F, Truong TN. Mechanisms for methane and ethane formation in the reaction of hydrogen with carbonaceous materials. Carbon 2005;43:1820-1827.
[30] Isobe S, Ichikawa T, Gottwald JI, Gomibuchi E, Fujii H. Catalytic effect of 3d transition metals on hydrogen storage properties in mechanically milled graphite. J. Phys. Chem. Solids 2004;65:535-539.
[31] Tölle J. Ti- oder Ti- und Fe- dotierte Natriumalanate als neue reversible Wasserstoffspeicermaterialien. Dissertation, Max-Planck-Institut für Kohlenforschung, Mülheim an der Ruhr 1998.
[32] Bogdanovic B, Brand RA, Marjanovic A, Schwickardi M, Tölle J. Metal-doped sodium aluminium hydrides as potential new hydrogen storage materials. J. Alloys Compd. 2000;302:36-58.
[33] ETHZ Merkblatt Batterien und Akkus. 2003. http://www2.ife.ee.ethz.ch/~rolfz/batak/Merkblatt_Batterien_und_Akkus.pdf; [viewed 23.06.2010]
[34] Johnson TA, Dedrick DE, Stephens RD, Chan JP. Sodium Alanate Hydrogen Storage Material. U.S. Patent.,Pub.-Nr. US 2007/0178042 A1. 2007.
[35] Gross KJ, Majzoub E, Thomas GJ, Sandrock G. Hydride development for hydrogen storage. Proceedings of 2002 U.S. DOE hydrogen program review (NREL/CP-610-32405). Golden, CO., 2002.
[36] Peters M, Leyens C. Titan und titanlegierungen. Weinheim: Wiley-VCH, 2002.
[37] Na Ranong C, Höhne M, Franzen J, Hapke J, Fieg G, Dornheim M. Modellgestützte verfahrenstechnische Berechnung eines Metallhydridspeichers auf Natriumalanatbasis im Technikumsmaßstab. Chemie Ingenieur Technik 2009;81:645-654.
[38] Na Ranong C, Hapke J, Höhne M, Fieg G, Bellosta von Colbe JM. Modelling and simulation of a large-scale metal-hydride storage tank on the basis of sodium alanate. 7th International Conference on Heat Transfer, Fluid Mechanics and Thermodynamics. Antalya, Turkey, 2010.
[39] Luo W, Gross KJ. A kinetics model of hydrogen absorption and desorption in Ti-doped NaAlH4. J. Alloys Compd. 2004;385:224-231.
[40] Tang X, Mosher DA, Anton DL. Practical sorption kinetics of TiCl3 catalyzed NaAlH4. Mater. Res. Soc. Symp. Proc. 2005;Vol 884E:GG4.4.
[41] Comsol Multiphysics Version 3.4. Computer Software, COMSOL AB. Copyright 1994-2007
[42] Na Ranong C, Lozano GA, Hapke J, Roetzel W, Fieg G, Bellosta von Colbe JM. Application of Danckwerts-type boundary conditions to the modeling of the thermal behavior of metal hydride reactors. Chem. Eng. Sci. 2010;submitted.

Appendix: Simulation model of sodium alanate material absorption

Previously, Franzen developed a numerical simulation for the absorption of sodium alanate [11], which was further extended by Na Ranong for the development of a prototype tank based on sodium alanate [13, 37, 38]. Based on these works, a numerical simulation for the present investigation was further developed. It uses a new empirical kinetic model for hydrogen absorption of sodium alanate material [23, 24] and a new approach for the material balance, which eliminates the use of artificial terms in the kinetic equations (as done in other kinetic models [11, 13, 39, 40])**.** The numerical simulation of the coupled sub-processes is implemented and solved in COMSOL^{TM}, a software package that solves partial differential equations by the finite element method [41]. The proposed modeling approach is not restricted to sodium alanate material and is also suitable for simulation of other metal hydride systems.

For the simulations of the present paper the cross-section of the tubular tank presented in Fig. 1 is considered. The physical phenomena to be simulated are hydrogen transport, intrinsic kinetics and heat transfer. The discussion about the governing equations for hydrogen transport and heat transfer and the corresponding boundary conditions can be founded elsewhere [37, 42]. Here the new approach for modeling the intrinsic kinetics of the hydrogen absorption process of sodium alanate material is addressed.

Intrinsic kinetics determines the local rate of reaction in which the chemical transformation proceeds, depending on the local hydrogen pressure, temperature and composition in the hydride bed. To describe and follow this transformation, a new approach is proposed in this investigation, in which the hydride bed of sodium alanate is considered as a mixture of three types of material that composes the reacting system. Their mass concentrations are used to follow the physical phenomena in the simulation. The mass concentration of a component in the mixture corresponds to its mass divided by the volume of the mixture. As indicated in [23], some fraction of the reacting material is inert during the second absorption step. Table 3 shows the mass fraction of the material used in this investigation according to the obtained experimental results. The mass concentrations of each type of material are also presented, which are calculated from their mass fractions and for the case of loose material (experimental bulk density of 0.6 g ml^{-1}). It is assumed that in the initial conditions of the absorption simulation all material is in the desorbed state.

Table 3: Mass fraction and mass concentration of the different type of materials that compose the initial sodium alanate material mixture according to experimental results [23, 24]. Bulk density of the initial sodium alanate material mixture is 0.6 g ml^{-1}.

Type of Material	Mass fraction [-]	Mass concentration [kg m^{-3}]
Active material for both absorption steps	0.5805	348.3
Active material for the first absorption step only	0.2271	136.3
Inert material	0.1924	115.4

The reacting system is modeled as two consecutive absorption steps and only their net rate of reaction is considered. Eq. 4 and 5 define the stoichiometry of the first and second absorption steps, respectively. Eq. 4 includes the additional aluminum and hydrogen required for the second absorption step, Eq. 5.

$$3NaH + 3Al + 4.5H_2 \rightarrow Na_3AlH_6 + 2Al + 3H_2 \quad (4)$$

$$Na_3AlH_6 + 2Al + 3H_2 \rightarrow 3NaAlH_4 \quad (5)$$

Three mixtures of defined composition are used to describe the reacting system (Tang et al. [40] proposed a similar definition)

$$S_I = 3NaH + 3Al + 4.5H_2 \quad (6)$$

$$S_{II} = Na_3AlH_6 + 2Al + 3H_2 \quad (7)$$

$$S_{III} = 3NaAlH_4 \quad (8)$$

Eq. 9 represents the absorption reacting system as defined in Eqs. 4 to 8. The stoichiometry for the numerical simulation is followed per unit of volume, e.g. in terms of mass concentrations of the materials. It is assumed that the bulk volume of the hydride bed is constant. Eq. 10 to 12 are the fundamental model equations for the finite element absorption simulation. Eq. 13 and 14 are expressions of the instantaneous rate of absorption in terms of mass concentrations based on a developed empirical kinetic model for sodium alanate absorption [23].

$$S_I \xrightarrow{r'_{a1}} S_{II} \xrightarrow{r'_{a2}} S_{III} \quad (9)$$

$$\frac{d\gamma_{S_I}}{dt} = -r'_{a1} \quad (10)$$

$$\frac{d\gamma_{S_{II}}}{dt} = r'_{a1} - r'_{a2} \quad (11)$$

$$\frac{d\gamma_{S_{III}}}{dt} = r'_{a2} \tag{12}$$

$$r'_{a1} = 1.33 k_{S_I \rightarrow S_{II}} \gamma_{S_I} \left\{ \ln\left(\frac{\gamma_{S_I} + \gamma_{S_{II}}}{\gamma_{S_I}} \right) \right\}^{0.25} \tag{13}$$

$$r'_{a2} = 1.33 k_{S_{II} \rightarrow S_{III}} \gamma_{S_{II}} \left\{ \ln\left(\frac{\gamma_{S_{II}} + \gamma_{S_{III}}}{\gamma_{S_{II}}} \right) \right\}^{0.25} \tag{14}$$

From the stoichiometry of the system, the volumetric rate of hydrogen absorption (kg m^{-3} s^{-1}) is calculated using Eq. 15. The volumetric heat of reaction (J m^{-3} s^{-1}) is calculated using Eq. 16, which corresponds to the expression of the source term required for the governing equation of heat transfer in the hydride bed.

$$r'_{abs} = r'_{a1} \left(\frac{\Delta m_{H_2}}{\Delta m_{S_I}} \right)_{S_I \rightarrow S_{II}} + r'_{a2} \left(\frac{\Delta m_{H_2}}{\Delta m_{S_{II}}} \right)_{S_{II} \rightarrow S_{III}} = 0.0187 r'_{a1} + 0.0374 r'_{a2} \tag{15}$$

$$r'_{abs} \left(\frac{-\Delta H_R}{MW_{H_2}} \right) = r'_{a1} \left(\frac{\Delta m_{H_2}}{\Delta m_{S_I}} \right)_{S_I \rightarrow S_{II}} \left(\frac{-\Delta H_{R,S_I \rightarrow S_{II}}}{MW_{H_2}} \right) + r'_{a2} \left(\frac{\Delta m_{H_2}}{\Delta m_{S_{II}}} \right)_{S_{II} \rightarrow S_{III}} \left(\frac{-\Delta H_{R,S_{II} \rightarrow S_{III}}}{MW_{H_2}} \right) \tag{16}$$

The model equations of intrinsic kinetics are implemented in the simulation for the active material for both absorption steps, and for the active material for the first absorption step only (see Table 3). For material active during the two absorptions steps Eqs. 10 and 11 are solved. The mass concentration for this type of material is calculated on the basis of the mass conservation:

$$\left(\gamma_{S_I} + \gamma_{S_{II}} + \gamma_{S_{III}} \right)_t = \left(\gamma_{S_I} + \gamma_{S_{II}} + \gamma_{S_{III}} \right)_{t_0} = \text{Constant} \tag{17}$$

For material active during the first step of absorption, but inert to the second one, only Eq. 10 is solved. For this material, the relation $\gamma_{S_{III}} = 0$ is valid at any time. Therefore, the concentration $\gamma_{S_{II}}$ can be calculated directly from the mass conservation equation (Eq. 17).

The solid density, bulk density and porosity of the material, needed during the modeling of the system, are calculated from the mass concentrations as shown in Eqs. 18 to 20. The hydrogen-free mass concentrations, γ^0, are based on the stoichiometry definitions of S_I, S_{II} and S_{III}, see Eqs. 21 to 23

$$\rho_s = \frac{\gamma^0_{S_I} + \gamma^0_{S_{II}} + \gamma^0_{S_{III}} + \gamma_{Inerts}}{\frac{\gamma^0_{S_I}}{\rho^0_{S_I}} + \frac{\gamma^0_{S_{II}}}{\rho^0_{S_{II}}} + \frac{\gamma^0_{S_{III}}}{\rho^0_{S_{III}}} + \frac{\gamma_{Inerts}}{\rho_{Inerts}}} \tag{18}$$

$$\rho_b = \gamma^0_{S_I} + \gamma^0_{S_{II}} + \gamma^0_{S_{III}} + \gamma_{Inerts} \tag{19}$$

$$\varepsilon = 1 - \frac{\rho_b}{\rho_s} \tag{20}$$

$$\gamma_{S_I}^0 = 0.9439\gamma_{S_I} \tag{21}$$

$$\gamma_{S_{II}}^0 = 0.9626\gamma_{S_I} \tag{22}$$

$$\gamma_{S_{III}}^0 = \gamma_{S_{III}} \tag{23}$$

Nomenclature

D_a	[mm]	external diameter of the tubular tank
D_i	[mm]	internal diameter of the tubular tank
D_{sf}	[mm]	external diameter of the sintered metal filter
k	[s^{-1}]	rate constant
K	[N mm^{-2}]	design strength value of the wall material
L	[m]	total length of the tubular tank
m	[kg]	mass
$m_{H_2,10\,min}$	[kg]	mass of hydrogen absorbed after 10 min
$m_{H_2,tot}$	[kg]	total mass of hydrogen that can be absorbed by the material
MW	[kg mol^{-1}]	molar mass
p	[bar]	pressure
r'	[kg m^{-3} s^{-1}]	hydrogen sorption rate per bulk volume of reacting material
r'_{a1}	[kg m^{-3} s^{-1}]	net rate of the first absorption step per bulk volume of reacting material
r'_{a2}	[kg m^{-3} s^{-1}]	net rate of the second absorption step per bulk volume of reacting material
s	[mm]	required wall thickness
S	[-]	design safety factor

S_I	[-]	mixture of 3 mol NaH, 3 mol Al, and 9/2 mol H_2
S_{II}	[-]	mixture of 1 mol Na_3AlH_6, 3 mol Al, and 3 mol H_2
S_{III}	[-]	3 mol $NaAlH_4$
t	[s]	time
t_0	[s]	initial time
$w_{10\,\mathrm{min}}$	[-]	mass of hydrogen absorbed after 10 minutes per mass of material
w_{tot}	[-]	total mass of hydrogen that can be absorbed by the material per mass of material

Greek

ΔH_R	[J mol H_2^{-1}]	enthalpy of reaction per mol of hydrogen
γ	[kg m^{-3}]	mass concentration
γ^0	[kg m^{-3}]	hydrogen-free mass concentration
ε	[-]	porosity of the hydride bed
κ	[m^2]	permeability of the hydride bed
ρ^0	[kg m^{-3}]	hydrogen-free density
ρ_b	[kg m^{-3}]	bulk density
ρ_s	[kg m^{-3}]	solid density

Subindixes

abs	absorption (hydrogenation)

Abbreviations

EG	expanded graphite
H_2	molecular hydrogen